

Photoluminescence study of a bimodal size distribution of Ge/Si(001) quantum dots

V. Yam,¹ Vinh Le Thanh,^{1,*} Y. Zheng,² P. Boucaud,¹ and D. Bouchier¹

¹*Institut d'Électronique Fondamentale, UMR-CNRS 8622, Bâtiment 220, Université Paris-Sud, 91405 Orsay Cedex, France*

²*Laboratoire Minéralogie-Cristallographie, URA-CNRS 09, Université Paris VI, 4-Place Jussieu, 75252 Paris Cedex 5, France*

(Received 28 July 2000; published 2 January 2001)

This work presents a study on the effect of a bimodal size distribution and of the pyramid/dome transition to the optical properties of self-assembled Ge/Si quantum dots. The wetting layers are shown to be inhomogeneous in thickness due to lateral diffusion of Ge from two-dimensional (2D) layers towards islands of bimodal sizes, while the island-related photoluminescence remains unchanged. The results indicate that three-dimensional islands, at their early stages of nucleation, are formed by consuming Ge from 2D layers and that the island luminescence energies are more sensitive to Ge/Si interdiffusion than the confinement effect inside the islands as currently believed.

DOI: 10.1103/PhysRevB.63.033313

PACS number(s): 68.65.-k, 85.35.Be, 05.65.+b, 78.66.-w

Over the last few years, the self-assembled technique, which takes advantage of the strain-driven two- to three-dimensional (3D) growth mode transition, has received considerable attention since it could allow one to produce quantum-sized islands without needing any kind of mask or patterning.¹ The island size distribution, in view of their application as quantum dots in novel devices, is one of the most critical parameters that needs to be controlled and has been a subject of numerous investigations.²⁻¹⁵

A result of particular interest is the observation of a bimodal distribution of island sizes at high growth temperatures.³⁻¹¹ Small islands are typically square-based pyramids formed by four {105} facets while larger islands are multifaceted domes. The pyramids are metastable and have been shown to transform to domes with increasing the Ge coverage^{8,9} or after annealing.^{3-5,7,11} However, most previous works have been mainly focused on the structural aspect of the island-shape transition, and very little attention has been paid to the optical behavior resulting from this shape transition.

We study, in this work, the effect of the bimodal size distribution and of the island-shape transition on the optical properties of related layers. We have combined, for this purpose, optical characterizations by photoluminescence spectroscopy (PL) with structural characterizations by *in situ* reflection high-energy electron diffraction (RHEED) and atomic-force microscopy (AFM) on comparable samples.

Experiments were carried out in an ultrahigh-vacuum chemical-vapor deposition (UHV-CVD) system. Pure SiH₄ and hydrogen-diluted (10%) GeH₄ were used as gas sources. The system has a base pressure better than 1×10^{-10} Torr, and the pressure during growth was about 5×10^{-4} Torr. The growth chamber is equipped with a differentially pumped RHEED system, allowing us to probe the growing surface even at high partial pressures of hydrides. Ge deposition was carried out at 700 °C to ensure the formation of bimodal size islands. The Ge growth rate, estimated from RHEED oscillations at 550 °C, is 1.5 monolayers (ML)/min. Details of the experimental setup and growth conditions can be found elsewhere.¹²

Figure 1(a) shows a typical AFM image of a sample obtained just after the onset of the island formation determined

from RHEED. The Ge growth time is 160 s, corresponding to a critical thickness of 4 ML s. The surface exhibits islands with two different sizes and shapes, in agreement with previous works.^{3-5,7-10} The domed islands have an average size of 115 nm and a height of 22 nm, while the pyramidal islands have an average width of 103 nm and a height of 11.7 nm. The aspect ratio of the domes is ~ 0.19 , almost twice as large as that of the pyramids. It is worth noting that the pyramids observed here have {104} and {103} facets depending on the island size, in comparison to the {105} facets reported in the literature (the tilt angles determined from AFM height profile are, respectively, $\sim 14^\circ$ and 18° instead of 11° for {105} facets). We note that in the growth conditions used in the present work, the {105} facets are only observed for ‘‘hut’’ clusters, i.e., for islands grown at low temperatures. The huts are very flat and have in general an elongated base and a high density, compared to a squared base and a low density of pyramidal islands formed at high growth temperatures.

The evolution of the PL spectrum of a Ge layer when the Ge coverage (θ_{Ge}) increases from 2.4 to 9 ML is displayed in Fig. 1(b). The spectra in the shadow part correspond to the 2D RHEED growth regime while those in the upper part correspond to the islanding mode. Apart from the PL line at 1098 meV, which is originated from the Si substrate and capped layers, the sample spectra with θ_{Ge} below 2.8 ML *only* exhibit two main lines, labeled NP_{WL} and TO_{WL}, which are, respectively, attributed to the no-phonon line and its TO-phonon replica of the narrow Ge quantum well.^{6,13-15} The energy difference between the NP and TO lines is $\sim 57-58$ meV, which corresponds to the Si-Si optical phonon energy in Si.¹⁶ The spectra for $\theta_{\text{Ge}}=3$ and 3.5 ML are dominated by an intense and very broad line, while the wetting-layer (WL) component has almost disappeared. This line has been attributed to intermediate clusters between 2D layers and 3D islands¹⁷ and is not the subject of the present work. For samples obtained after the 2D-3D transition ($\theta_{\text{Ge}} \geq 4$ ML), the spectra exhibit two separate components that correspond to the Ge (WL's) and Ge islands, respectively. The component at higher energies stems from the WL's while the two broader peaks observed at energies below 860 meV, denoted at this moment as NP_i and TO_i, can be attributed to 3D islands.

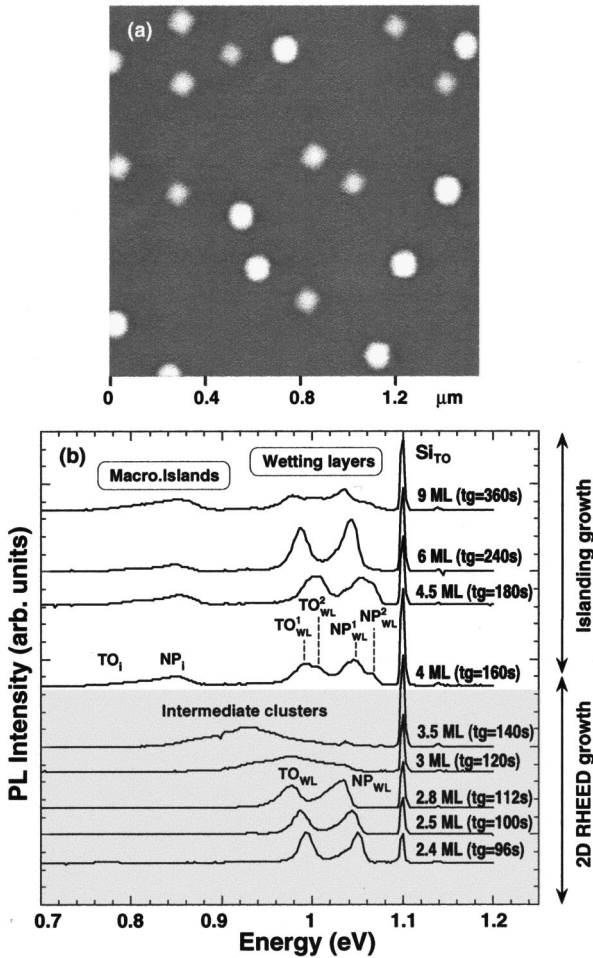


FIG. 1. (a) Typical AFM image exhibiting islands with two different sizes and shapes. Small islands are square-based pyramids formed by {104} and {103} facets while larger islands are multifaceted domes. (b) 11-K PL spectra illustrating different stages of Ge growth with increasing θ_{Ge} . The growth temperature is 700 °C.

Compared to the WL component observed in the 2D growth regime (for $\theta_{\text{Ge}} \leq 2.8$ ML), the WL component obtained for $\theta_{\text{Ge}} = 4$ and 4.5 ML exhibits two different features. First, it exhibits a blueshift when θ_{Ge} increases from 4 to 4.5 ML and then a redshift with further increase of θ_{Ge} from 6 to 9 ML. The blueshift has been previously observed and has been explained as being due to a Ge lateral diffusion from 2D layers towards islands.^{13–15} The redshift is, on the other hand, observed for the first time and its origin will be discussed later. Second and more importantly, the WL component now contains four main lines, denoted to as NP_{WL}^1 , TO_{WL}^1 , NP_{WL}^2 , and TO_{WL}^2 , instead of the two lines observed in the 2D growth regime. Interestingly, the separation in energy between these two pairs of lines, ($\text{NP}_{\text{WL}}^1, \text{TO}_{\text{WL}}^1$) and ($\text{NP}_{\text{WL}}^2, \text{TO}_{\text{WL}}^2$), is still $\sim 57\text{--}58$ meV, a value expected for the energy separation between the NP and TO lines of a pseudomorphic 2D Ge layer. The coexistence of these two pairs of lines therefore indicates that the Ge WL's in between the islands are not uniform but consist at least of two different thicknesses. Comparison of this result with bimodal size islands observed in Fig. 1(a) appears to show that the presence of these two pairs of lines arises from the Ge lateral

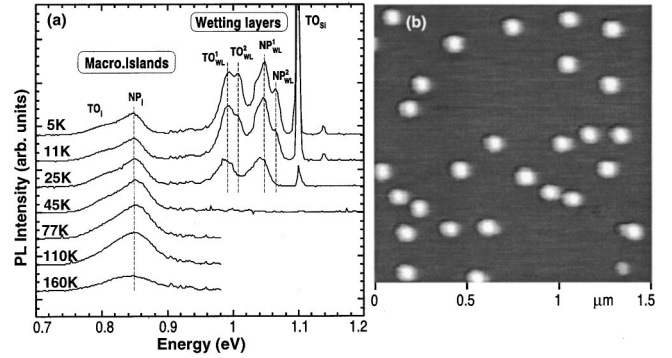


FIG. 2. (a) PL temperature dependence for a sample with $\theta_{\text{Ge}} = 4$ ML. (b) AFM image of a sample surface with $\theta_{\text{Ge}} = 6$ ML; the growth temperature is 700 °C. The image reveals the presence of only dome-shaped islands, indicating that the pyramidal islands are no longer stable.

diffusion from the 2D layers towards the islands having two different sizes.

To further investigate the influence of the bimodal size distribution on the WL-related PL, we have measured the PL temperature dependence for the sample with $\theta_{\text{Ge}} = 4$ ML. The result is depicted in Fig. 2(a). With increasing the temperature, the intensity of both NP_{WL}^2 and TO_{WL}^2 lines is found to decrease more rapidly than that of the ($\text{NP}_{\text{WL}}^1, \text{TO}_{\text{WL}}^1$) lines. At a temperature of about 25 K, only the ($\text{NP}_{\text{WL}}^1, \text{TO}_{\text{WL}}^1$) pair persists while the ($\text{NP}_{\text{WL}}^2, \text{TO}_{\text{WL}}^2$) pair is completely quenched. Since the temperature quenching of the WL PL is mainly due to the thermionic emission of the carriers from the Ge wells to the Si barrier, the above results support the idea of the existence of two WL thicknesses. Indeed, because a larger quantum well has a smaller confinement energy, when the temperature increases the thermionic emission of the carriers towards the Si barriers will first occur for the less deep levels, i.e., for the thinner quantum well. The PL of the larger well in which the carriers are more deeply confined is maintained at higher temperatures.

Let us now consider the effect of a bimodal size distribution on the island-related PL. Since the PL of the islands consists of two peaks, there has been a suggestion that these two peaks might originate from the bimodal size distribution.¹⁸ However, if each of these two peaks originates from one kind of island (a high-energy peak from pyramids and a low-energy from domes), it is expected that the thermionic emission of the carriers towards the Si barriers will first occur for the peak located at the high-energy side due to a lower barrier potential towards Si. This is not what is observed experimentally. As can be seen in Fig. 2(a), when the temperature increases, the lower-energy peak is quenched at about 77 K while the high-energy peak persists up to much higher temperatures.

Another point that may allow us to understand the island-related PL of bimodal size islands is to determine the Ge coverage at which the transition from pyramids to domes occurs. The surface, which is obtained just after the pyramid/dome transition, is expected to exhibit islands with a very narrow size distribution. We have then undertaken systematic investigations of the surface morphology with the Ge coverage increasing from 4 to 9 ML. Figure 2(b) shows an

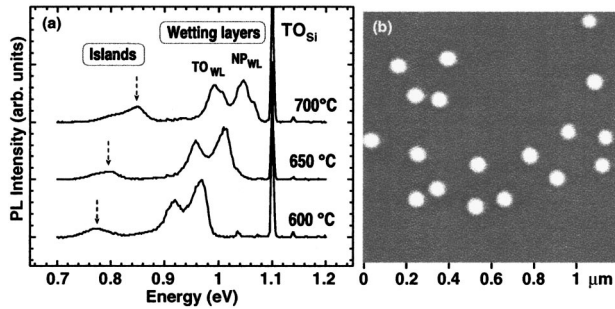


FIG. 3. (a) Typical 11-K PL spectra of samples grown at 650 and 600 °C. The Ge coverage is 4 ML. (b) AFM image of a sample surface with $\theta_{\text{Ge}}=4$ ML, the growth temperature is 600 °C.

AFM image of a sample surface with $\theta_{\text{Ge}}=6$ ML. The image reveals the presence of only dome-shaped islands, indicating that the pyramidal islands are no longer stable. The islands are very uniform; their dimensions are ~ 120 nm in size and 30 nm in height. Interestingly, as can be seen in Fig. 1(b) the island-related PL does not exhibit any changes, neither in the peak shape nor in the energy positions, as θ_{Ge} increases from 4 up to 9 ML. This result unambiguously rules out the possibility that each of these two peaks originates from one kind of island. These two peaks can be therefore attributed to the NP and TO phonon-assisted transitions inside the ensemble of islands. In this regard, these two peaks are denoted to as NP_i and TO_i . We also note that the WL component of the corresponding sample ($\theta_{\text{Ge}}=6$ ML) exhibits only one ($\text{NP}_{\text{WL}}, \text{TO}_{\text{WL}}$) pair, confirming that the coexistence of two ($\text{NP}_{\text{WL}}, \text{TO}_{\text{WL}}$) pairs arises from a bimodal size distribution observed at $\theta_{\text{Ge}}=4$ and 4.5 ML.

We now comment on the relationship between the island dimensions and the luminescence energies. First, it is worth noting that the lateral sizes of 3D islands are more than 100 nm, a value which appears too large to induce lateral confinement. The confinement energy, if there exists, might stem from vertical confinement effect. However, as can be seen above, the energy positions of the island PL remain almost unchanged when the average island heights vary from 11.7 nm at $\theta_{\text{Ge}}=4$ ML up to 30 nm for $\theta_{\text{Ge}}=6$ ML. This suggests that such island heights are already too large to induce vertical confinement.

To determine the main parameters that might govern the island-PL energy, we have undertaken Ge growth at various growth temperatures. Shown in Fig. 3(a) are typical PL spectra obtained for growth temperatures of 650 and 600 °C. For comparison, we report in the upper figure the PL spectrum of a sample with $\theta_{\text{Ge}}=4$ ML grown at 700 °C. We note that in all cases the Ge deposition was stopped just after the RHEED 2D-3D transition, i.e., the Ge coverage is equal to the critical thickness. The figure clearly shows that the island-related PL shifts to lower energies when the growth temperature decreases. The island-related NP_i line, which is observed at 850 meV for a growth temperature of 700 °C, is found to decrease to 800 and 775 meV at 650 and 600 °C, respectively. On the other hand, AFM measurements on the corresponding samples indicate that both island size and heights decrease with decreasing growth temperature from 700 to 600 °C. An example for the sample grown at 600 °C is

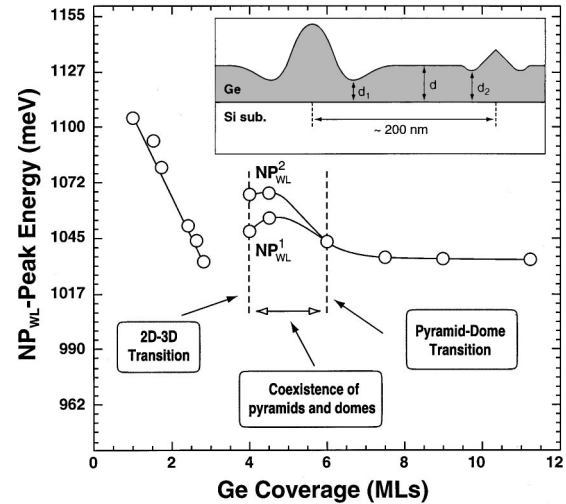


FIG. 4. Variation of the energy position of WL NP peaks with increasing θ_{Ge} . Note that for $\theta_{\text{Ge}}=3-4$ ML the WL PL is quenched due to an efficient transfer of the carriers from the WL's to intermediate clusters. Shown in the inset is a scheme describing the variation of the WL thickness after the onset of the island formation.

shown in Fig. 3(b). The surface exhibits dome-shaped islands, whose dimensions are about 100 nm in size and 14–15 nm in height. The observed redshift of the island-related component together with the decrease of the island dimensions when the growth temperature decreases clearly indicate that the island luminescence energies are mainly determined by the degree of Si/Ge interdiffusion, which in turn depends on the growth temperature.

Based on the above optical and structural results, we will now discuss the kinetic pathways of the island formation. The different stages of the island formation and the variation of the energy position of the WL NP peaks with increasing the Ge coverage are summarized in Fig. 4. First, it is shown from the optical properties that when the Ge coverage reaches the critical thickness, which corresponds to the RHEED 2D-3D transition and of about 4 ML in this case, macroscopic islands are spontaneously formed. From the energy point of view, the spontaneous formation of 3D islands can be explained by the fact that at the critical thickness the built-in strain energy in the 2D layers becomes so high that the system should relax this energy. Islanding growth is known to be energetically favorable because it allows a partial relaxation of the strain by elastic deformation of the epilayers and substrate.¹⁹

The above results provide evidence that at the critical thickness 3D islands are spontaneously formed by consuming Ge from the 2D layers. This results in a reduction of the thickness of the wetting layers. This stage of the island formation can be considered as a nucleation process. We note that the blueshift of the WL component has been previously observed.^{13–15} However, experiments carried out on well-controlled bimodal size islands in which the amount of consumed Ge was shown to depend on the island volume confirm, on the one hand, the above picture of the island nucleation, and indicate, in the other hand, that the reduction amount of the WL thickness is kinetically controlled. Indeed, there has been a suggestion that the thickness of the wetting

layers that remained after the onset of the island formation is thermodynamically stable and corresponds the equilibrium critical thickness.¹³ Our above results clearly indicate that this thickness is not stable but depends on the island size and also on the evolution stage of the island formation.

It is interesting to note that the reduction of the WL thickness should contribute to the minimization of the total free energy of the system after the onset of the island formation. As the island formation increases the surface area, theoretical calculations of the total free energy of the system were only based on the balance in energy between the increase of the surface free energy and the reduction of the strain energy by elastic relaxation while the thickness of the 2D layers was assumed unchanged.¹⁹ However, as can be seen in Figs. 1 and 4, after the onset of the island formation the energy position of the NP_{WL}^2 line is 1067 meV. This value, estimated from calculations of the confinement energy in a square-well potential with the data obtained in the 2D growth regime, corresponds to a thickness of about 2.2 ML. This means that for 4 ML of deposited Ge, almost 2 ML has been consumed to form islands. In other words, the elastic energy of the remaining 2D layers has been reduced by a factor of almost 2 after the onset of the island formation.

We note that at 700 °C, alloying between the Ge and the Si substrate and Si cap layer should occur. Furthermore, it has been shown that alloying is greatly enhanced by strain, i.e., near or on the islands.²⁰ However, since islands are typically 200 nm apart, it appears reasonable to assume that intermixing in the wetting layers (WL's) after the onset of the island formation has a degree comparable to that in the 2D layers obtained with θ_{Ge} below 4 ML.

The thinning of the WL thickness is observed for θ_{Ge} increasing to 4.5 ML, suggesting that the nucleation process is spread out up to this coverage. For a further increase of the Ge coverage to 6 ML, the WL component is found to exhibit a shift to lower energies. It is worth noting that at this coverage, AFM measurements have revealed a shape transition from pyramids to domes [Fig. 2(b)]. Such an evolution can be explained by the fact that after the nucleation stage, the thickness of the wetting layers has been thinned. Therefore, with further deposition of Ge, a part of this will go to the wetting layers, resulting in a redshift of the WL component. This result suggests that with increasing the Ge coverage a new stage of the island formation, termed island growth,

starts. The redshift of the WL component is observed for θ_{Ge} increasing up to 9 ML and then remains unchanged for a further increase of θ_{Ge} up to about 14 ML. AFM measurements reveal that at $\theta_{\text{Ge}}=9$ ML, island coalescence starts, resulting in the formation of multimodal size islands. The disappearance of the WL component for $\theta_{\text{Ge}}\geq 14$ ML may be associated with the appearance of dislocations at the edge of coalesced islands whose sizes become larger than 600 nm.

The last point meriting comment is why only two pairs of lines related to the WL's are observable from PL. As can be seen in the inset of Fig. 4, the WL's may present three thicknesses: a WL having an average thickness (d) on which islands typically 200 nm apart are linked; this thickness, due to the lateral diffusion of Ge from 2D layers towards islands, is reduced to d_1 and d_2 in the vicinity of domes and pyramids, respectively. d_1 is smaller than d_2 because the volume of domes is almost twice as large as that of the pyramids. Since only two WL thicknesses are observable, the pair observed at higher energies, ($\text{NP}_{\text{WL}}^2, \text{TO}_{\text{WL}}^2$), can be attributed to the thinnest thickness (d_1), while the other pair, ($\text{NP}_{\text{WL}}^1, \text{TO}_{\text{WL}}^1$), may stem from the largest one (d). The thickness d_2 , which is between d and d_1 , may manifest itself in a broadening of the PL lines.

In summary, we have studied the effect of a bimodal size distribution and of the pyramid/dome transition to the optical properties of related Ge/Si layers. By combining structural with optical characterizations, three stages of the island formation can be identified with increasing Ge coverage: island nucleation, island growth, and finally island coalescence. It is worth noting that the above reported value of the Ge coverage corresponding to each growth stage represents only a relative character. It should depend on the degree of Ge/Si intermixing and the Ge flux. We have shown that when the thickness of the 2D layers reaches the critical thickness, the island nucleation takes place by consuming Ge from the 2D layers. The shape transition from pyramids to domes corresponds to the island growth stage that occurs just after the nucleation stage. Concerning the island optical properties, though much remains to be done in order to establish the relationship between the island-related luminescence energies and the island dimensions, the present work reveals the surprising result that the island luminescence energies appear to be more sensitive to the Ge/Si interdiffusion than the confinement effect.

*Author to whom correspondence should be addressed. Email: lethanh@ief.u-psud.fr

¹D. J. Eaglesham and M. Cerullo, Phys. Rev. Lett. **64**, 1943 (1990).

²M. Goryll *et al.*, Appl. Phys. Lett. **71**, 410 (1997).

³T. I. Kamins *et al.*, J. Appl. Phys. **81**, 211 (1997).

⁴J. A. Floro *et al.*, Phys. Rev. Lett. **80**, 4717 (1998).

⁵G. Medeiros-Ribeiro *et al.*, Science **279**, 353 (1998).

⁶V. Le Thanh *et al.*, Phys. Rev. B **58**, 13 115 (1998).

⁷T. I. Kamins *et al.*, J. Appl. Phys. **85**, 1159 (1999).

⁸F. M. Ross *et al.*, Phys. Rev. Lett. **80**, 984 (1998).

⁹F. M. Ross *et al.*, Science **286**, 1931 (1999).

¹⁰O. G. Schmidt *et al.*, Appl. Phys. Lett. **75**, 1905 (1999).

¹¹C. P. Liu *et al.*, Phys. Rev. Lett. **84**, 1958 (2000).

¹²V. Le Thanh *et al.*, Phys. Rev. B **60**, 5851 (1999).

¹³H. Sunamura *et al.*, Appl. Phys. Lett. **66**, 3024 (1995).

¹⁴P. Schittenhelm *et al.*, Appl. Phys. Lett. **67**, 1292 (1995).

¹⁵G. Abstreiter *et al.*, Semicond. Sci. Technol. **11**, 1521 (1996).

¹⁶J. Weber and M. I. Alonso, Phys. Rev. B **40**, 5683 (1989).

¹⁷V. Le Thanh *et al.* (unpublished).

¹⁸O. G. Schmidt and K. Eberl, Phys. Rev. B **61**, 13 721 (2000).

¹⁹J. Tersoff and F. K. LeGoues, Phys. Rev. Lett. **72**, 3570 (1994).

²⁰S. A. Chaparro *et al.*, Phys. Rev. Lett. **83**, 1199 (1999); T. I. Kamins *et al.*, Appl. Phys. A: Mater. Sci. Process. **67**, 727 (1998).